Observation of second-order Stark effects in silane, SiH_4

W. A. Kreiner[a)]

Abteilung für Physikalische Chemie, Universität Ulm, D-7900 Ulm, West Germany

T. Oka

Herzberg Institute of Astrophysics, National Research Council of Canada, Ottawa, Ontario, Canada K1A OR6

A. G. Robiette

Department of Chemistry, The University, Reading RG6 2AD, England
(Received 11 November 1977)

The Stark effect on rovibrational transitions of the tetrahedral molecule silane has been studied by laser Stark spectroscopy, i.e., by applying dc fields of up to 65 kV/cm and monitoring the absorption of fixed frequency ir laser lines. The coincidences observed occur between the ν_4 fundamental of SiH_4 and N_2O laser lines. Using the inverse Lamb dip technique single M components of three high J transitions could be resolved, and two of these have been identified by rf–ir double resonance. In both cases the Stark shift is due to the second-order Stark mixing of A_1 with A_2 rotational levels. The analysis of the Stark effects is consistent with the ground state centrifugal distortion moment $\theta_z^{xy} = 3.34 \times 10^{-5}$ D measured previously by Kagann, Ozier, and Gerry. Experiments to measure the frequency offset $\Delta\nu = \nu_M - \nu_L$ of the molecular absorption lines from the nearest laser line have also been performed, using the beat between two N_2O lasers. Direct evidence of the second-order Stark shift has been obtained by observing Stark Lamb dips with a continuously tuned laser.

I. INTRODUCTION

Tetrahedral molecules attract increasing interest in the field of rotational spectroscopy, since the very small dipole moment generated in the ground vibrational state by centrifugal distortion has been studied by refined spectroscopic techniques (see Ref. 1 for a review of this field). A vibration-induced dipole moment is also present in the first excited state of infrared-active fundamentals,[2] but this effect has been the subject of fewer experiments.

Ozier[3] was able to measure the centrifugal distortion-induced dipole moment of CH_4 (denoted θ_z^{xy} by Watson[4]) by observing the Stark effect on a molecular beam magnetic resonance spectrum. This work provided the first experimental confirmation of the theory of the centrifugal distortion-induced dipole moment.[4–7] Subsequently, Kagann, Ozier, and Gerry[8] measured θ_z^{xy} for SiH_4 by observing the Stark effect on a pure rotation Q branch transition in a high-sensitivity microwave spectrometer, while Kreiner, Orr, Andresen, and Oka[9] investigated θ_z^{xy} for GeH_4 using three different laser techniques.

For all three molecules θ_z^{xy} is of the order 10^{-5} D. These small dipole moments give rise to Stark shifts which are correspondingly small. Attention has therefore centered on the levels whose rovibrational symmetry in T_d is E because these levels have a first-order Stark effect. Watson[10] has in fact shown that the E levels of T_d molecules are the only rovibrational levels of any nonpolar molecule to exhibit a first-order Stark effect. Although Uehara has reported an indication of a second-order effect for the excited state of CH_4,[11] it has generally been thought that the splitting of the M components of the second-order Stark shifts in the ground state levels with symmetry A_1, A_2, F_1, or F_2 in T_d would be too small to be observed in most experiments.

This paper is concerned with the interpretation of the laser Stark spectrum of SiH_4. In the extensive infrared vibration–rotation spectrum of SiH_4 in the 10 μm region, due to the Coriolis-coupled ν_2 and ν_4 bands, there are several near coincidences with N_2O and CO_2 laser lines.[12,13] Two silane lines which are near coincident with N_2O laser lines show strong resolvable laser Stark spectra: in each case the Stark shift is caused by the second-order Stark effect on an A_1 or an A_2 rovibrational level.

II. STARK LAMB DIP SPECTROSCOPY

A. Experimental method

The technique, which has now been applied to many molecules (see Ref. 9), consists of tuning the molecular absorption line into coincidence with a fixed-frequency laser line by the application of a dc electric field. In favorable circumstances several M components can be swept across the laser line.

A schematic diagram of the apparatus is shown in Fig. 1. Further details are given elsewhere.[14,15] The laser consists of a 2.5 m gain cell, with a concave mirror mounted on a piezo crystal at one end and a plane grating blazed at 10 μm at the other. The laser was stabilized to the center of the gain profile; the laser frequency varied by up to ± 2 MHz in different experiments. The direction of polarization could be changed through 90° by using a mirror combination.

The Stark electrodes consist of two polished steel plates, 40 cm long and separated by 1 mm quartz spacers. dc voltage of up to 6000 V was applied to one plate. A ramp voltage of opposite sign, modulated at 2 kHz by

[a)]N.R.C.C. Visiting Scientist Summer 1977.

 0021-9606/78/6807-3236$01.00

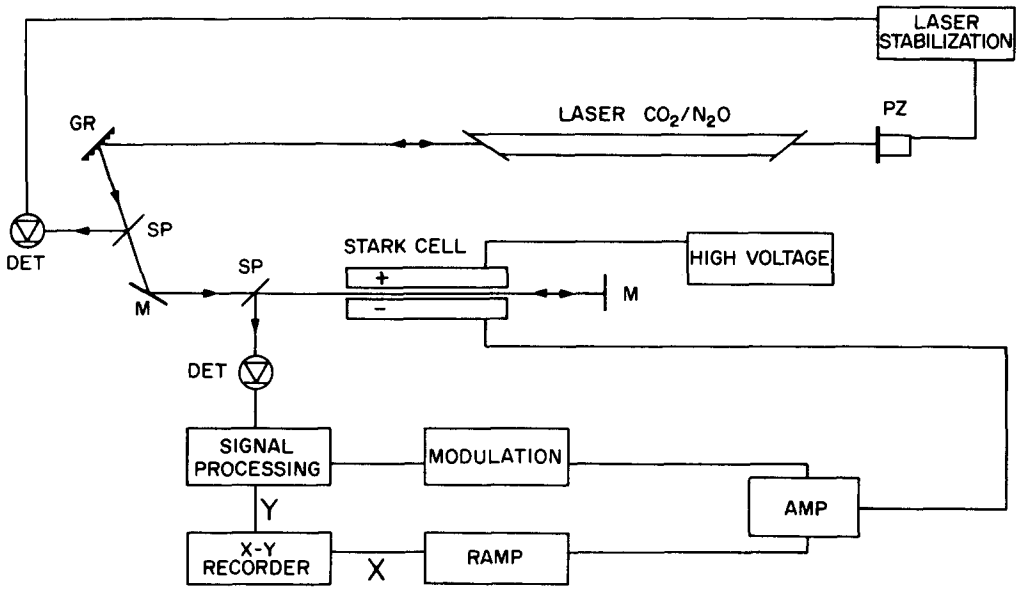

FIG. 1. Experimental arrangement for Stark effect measurements. The laser beam is reflected at the end of the cell for observation of the inverse Lamb dips of the Stark components.

up to 400 V peak to peak, was connected to the other electrode.

In order to observe Lamb dips the beam is reflected at the end of the Stark cell. Slight tilting of the mirror prevents the reflected beam from disturbing the laser. The frequency resolution is about 1 MHz, mainly limited by laser instabilities.

The absorption signal is monitored by a Pb–Sn–Te detector and fed into a phase-sensitive detector. $2f$ Detection was used because of its superior signal-to-noise ratio. As a result the second derivative of the line shape was observed.

B. Frequency offset measurements

In the conventional laser Stark experiment the spectrum gives the pattern of M components in the form of absorption plotted against electric field strength. The frequency scale of this pattern is not obtained and it must be established in separate experiments.

We carried out frequency measurements on the component of highest M for the two laser Stark spectra discussed below. Two N_2O lasers oscillating on the same line were used. One was locked to its center frequency, serving as a fixed-frequency local oscillator (reference laser), while the other was used to observe the laser Stark spectrum of SiH_4 (signal laser). The signal laser was set to different frequencies within its gain profile by tuning the cavity length. The frequency offset between signal and reference lasers was measured by directing out-coupled beams from both lasers to a second detector and monitoring the beat on a spectrum analyzer: the total tuning range was about ± 22 MHz from the reference laser. A similar experiment with CO_2 lasers has been described for GeH_4.[9]

By measuring the electric field needed to bring the component of highest M into resonance for each setting of the signal laser, we obtain the Stark effect of this component in the form of frequency shift as a function of electric field strength.

C. Continuous laser scanning

In an alternative experiment, the frequency of the laser was scanned over the Stark split lines by applying a sawtooth voltage to the piezoelectric crystal on which the end mirror is mounted. The maximum range of scanning was limited to 67 MHz determined by the longitudinal mode separation for the 225 cm laser cavity. The linearity of the scanning and the deviation from it were known from the previous experiment, thus enabling us to measure the laser frequency approximately. By using this method for the $R(18)$ transition, we could obtain the splitting pattern as a function of laser frequency. The electric field of the laser was parallel to that of the Stark field leading to observation of $\Delta M = 0$ transitions.

D. Results

Laser Stark spectra were observed with three N_2O laser lines, $P(25)$, $R(16)$, and $R(24)$. The spectrum associated with $P(25)$ was weak and has not been investigated in detail. Preliminary reports of the spectra associated with $R(16)$ and $R(24)$ have been given earlier.[1,12,13]

Figure 2 shows a sequence of M components obtained with the N_2O $R(16)$ line. In Fig. 2(a) the laser polarization is parallel to the electric field, giving rise to $\Delta M = 0$ transitions, while in Fig. 2(b) the laser polarization is perpendicular to the electric field, giving rise to $\Delta M = \pm 1$ transitions. The two traces are very similar. Repeated measurements of both types of transition indicated that within the accuracy of the laser stability they occur at the same electric field strengths. The same is true of the spectrum obtained with the N_2O $R(24)$ line. This led us to the conclusion that the Stark splitting in the upper state is extremely small, and that the Stark effect arises almost entirely from the ground state. Averaged measurements for the $\Delta M = 0$ transitions of both spectra are given in Table I. The plate spacing needed for the calculation of electric field was

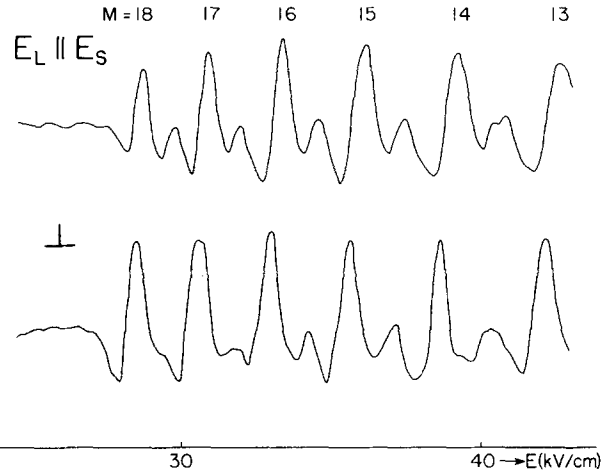

FIG. 2. Part of the inverse Lamb dip laser Stark spectrum of SiH_4, obtained with the N_2O $R(16)$ laser line. Absorption is shown as a function of electric field strength. E_L and E_S refer to the direction of the laser polarization and the Stark field respectively. Trace (a) shows $\Delta m = 0$ transitions, Trace (b) $\Delta m = \pm 1$ transitions. The small lines between the main components are believed to be the so-called center dips.[15]

determined sufficiently accurately by measuring the quartz spacers.

The small lines visible in Fig. 2 between the Lamb dips of the M components are believed to be the collision-induced center dips.[15]

The results of the frequency offset measurements are shown graphically in Fig. 3. It is clear that in both cases the Stark effect is approximately linear with applied electric field over the frequency range studied.

Figure 4 indicates the Stark pattern observed by a continuous scanning of the N_2O $R(16)$ laser line. The laser is oscillating over a range of 55 MHz. At the Stark field of 37.95 kV/cm, 13 Lamb dips are recorded. Owing to phase sensitive detection at the frequency of modulation, first derivative shapes of the Lamb dips are observed. The pattern clearly shows larger spacing for higher M components typical of a second-order Stark shift.

TABLE I. Observed and calculated resonance fields in the laser Stark spectrum of SiH_4.[a]

N_2O $R(16)$ laser line			N_2O $R(24)$ laser line		
$\lvert M \rvert$	ϵ_{obs}(kV cm^{-1})	ϵ_{calc}(kV cm^{-1})	$\lvert M \rvert$	ϵ_{obs}(kV cm^{-1})	ϵ_{calc}(kV cm^{-1})
18	30.15	30.19	21	34.60	34.64
17	31.98	31.96	20	36.36	36.37
16	33.90	33.96	19	38.29	38.28
15	36.19	36.22	18	40.42	40.41
14	38.81	38.81	17	42.74	42.79
13	41.81	41.80	16	45.45	45.46
12	45.23	45.28	15	48.62	48.49
11	49.16	49.40	14	52.11	51.96
10	54.05	54.34	13	56.25	55.95
9	60.03	60.37	12	60.71	60.62
Assumed parameters[b]					
θ_z^{xy}		3.34×10^{-5} D			3.34×10^{-5} D
$C(J,\kappa)$		17.605			20.285
$\Delta\nu_0$		993.062 MHz			859.088 MHz
Derived parameter[c]					
$\nu_M - \nu_L$		(+)25.4 ± 1 MHz			(−)66.5 ± 1 MHz

[a] ϵ_{calc} is obtained from the second-order Stark calculations described in Sec. III. C of text. The upper state Stark effect is assumed to be negligible.
[b] $\Delta\nu_0$ is the zero-field splitting between the A_1 and A_2 levels.
[c] $\nu_M - \nu_L$ is the difference between the molecular transition frequency and the laser frequency. The sign is derived from the frequency offset experiments shown in Fig. 2.

III. ASSIGNMENT AND CONFIRMATION BY DOUBLE RESONANCE

A. Comparison with the infrared spectrum

The ν_4 infrared band of SiH_4 was recorded at a resolution of ~ 0.06 cm^{-1} by Johns, Kreiner, and Susskind.[16]

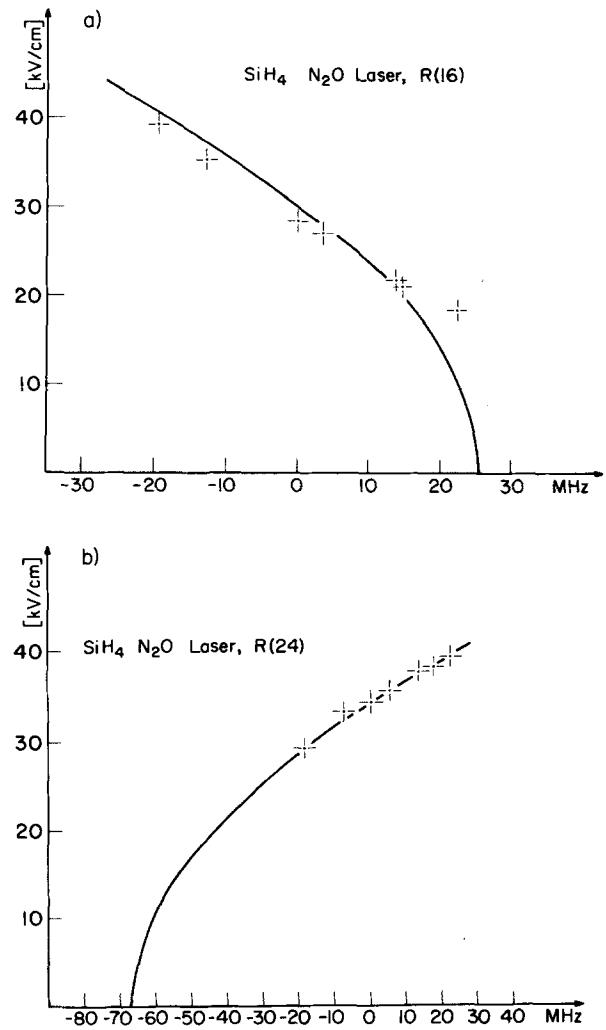

FIG. 3. Determination of the frequency shift of the component of highest M as a function of applied electric field. The field strength necessary to pull the fastest-moving Stark component into resonance with the signal laser (see text) is plotted against the frequency offset of the signal laser from its center frequency. The upper trace shows the measurements made with the N_2O $R(16)$ laser line [SiH_4 ν_4 $R^-(18)$ transition], the lower trace those made with the N_2O $R(24)$ laser line [SiH_4 ν_4 $R^-(21)$ transition]. The curves plotted on the graphs are the calculated second-order Stark shift of the ground-state levels alone, using the parameters of Table I. Note that the Stark shift, although parabolic at low fields, becomes approximately linear at fields of 30 kV/cm and above.

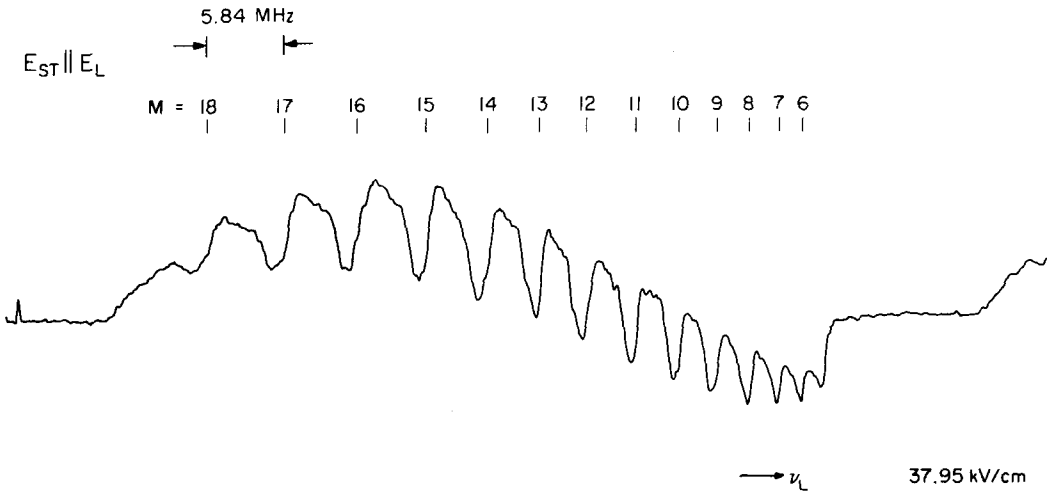

FIG. 4. Stark Lamb dips of the ν_4 $R^-(18)$ transition observed by scanning laser frequency. The N_2O $R(16)$ laser line was scanned about 55 MHz by changing the length of laser cavity.

They assigned the spectrum up to $J' = 12$ and achieved a partial fit of the transitions using Susskind's Hamiltonian.[17] Later this work was extended to include a recording of the ν_2 band, and by considering the Coriolis-coupled ν_2 and ν_4 bands together a good fit of the spectrum has been obtained up to $J' = 20$.[18] Thus it is now possible to use the infrared spectrum with confidence as an aid to assignment of the laser Stark spectra. Throughout we use the notation of the infrared study[18,19]; for the ground state energy levels this is the notation used by most of the recent papers.[12,20]

The pattern of M components as a function of electric field strength shows that the lower state J values of the two SiH_4 infrared transitions involved are 18 and 21, respectively, as assigned in Table I. [It should be emphasized that the product ϵm, where ϵ is the resonance electric field strength, is expected to be a constant whether the Stark shift is first or second order. This is a consequence of the form of the Stark matrix element connecting different rovibrational levels,

$$H_{\text{Stark}} = C(J, \kappa)\theta_g^{xy} m\epsilon ,$$

where $C(J, \kappa)$ is the Stark coefficient of Dorney and Watson.[20] If each M component in turn must be shifted by the same constant amount to bring it into coincidence with the laser line, it is clear the H_{Stark} must have the same value at resonance for all M values, regardless of whether it is a diagonal matrix element as in the first-order case or an off-diagonal matrix element as in the second-order case. The effect of Stark matrix elements between different J levels which do not have such simple M dependence is negligible in the present case.]

It was recognized at an early stage that the only transitions with these J values in this region of the infrared, 952.518 cm^{-1} for the N_2O $R(16)$ line and 958.602 cm^{-1} for the N_2O $R(24)$ line, are the strongly allowed R^- transitions of the SiH_4 ν_4 band.

The first assignment suggested for the N_2O $R(16)$ coincidence was ν_4 $R^-(18)$, $E^{(3)} - E^{(3)}$ of SiH_4,[1,12] but a double-resonance search for the connected ground-state transition $J = 18$, $E^{(3)} - E^{(2)}$ was unsuccessful. Furthermore, the detailed infrared analysis[18] showed that none of the $E - E$ components of $R^-(18)$ lies near the laser line. Instead, the infrared analysis suggested that the transitions most likely to coincide with the laser line are the three lines ν_4 $R^-(18)$, $A_2^{(2)} - A_1^{(2)}$, $F_2^{(4)} - F_1^{(4)}$ and $F_1^{(5)} - F_2^{(5)}$. These were calculated at 952.534 cm^{-1}, 952.571 cm^{-1}, and 952.615 cm^{-1}, respectively, and were observed as a single unresolved peak at 952.530 cm^{-1} [blended also with two strong $R^-(17)$ lines]. These possibilities could not be distinguished without further experiments.

In order to assign the N_2O $R(24)$ coincidence the theoretical prediction from the infrared constants was extended to $J' = 22$, enabling the ν_4 $R^-(20)$ and $R^-(21)$ transitions of SiH_4 to be calculated. The prediction was successful in that virtually all the strong infrared lines in the region 956 cm^{-1} to 967 cm^{-1} which were previously unassigned could be attributed to $R^-(20)$ and $R^-(21)$ transitions, the predictions falling mainly within about 0.05–0.08 cm^{-1} from the observed lines. The $R^-(21)$ transition closest to the laser line appeared to be ν_4 $R^-(21)$, $A_2^{(2)} - A_1^{(2)}$ of SiH_4, calculated at 958.552 cm^{-1} and observed at 958.596 cm^{-1}.

B. Confirmation by rf-ir double resonance

The rf–ir double resonance technique consists in placing a coaxial waveguide absorption cell inside the laser cavity.[12,21] If a high-power rf pump is applied to a rotational transition sharing a common level with an infrared transition within the Doppler profile of the laser, the laser acts as a monitor for the change in population density in the pumped level. Therefore, by sweeping the radio frequency, rotational transitions can be found by recording the laser output. We also obtained an indication of the Stark effect on the double resonance signals by applying a dc electric field to the coaxial cell, although the effect cannot be interpreted quantitatively because of inhomogeneity in the field.

For SiH_4 the energy level splittings in the ground vibrational state are known with considerable precision from the microwave work of Özier, Lees, and Gerry.[22] Their paper tabulates these splittings up to $J = 20$, with

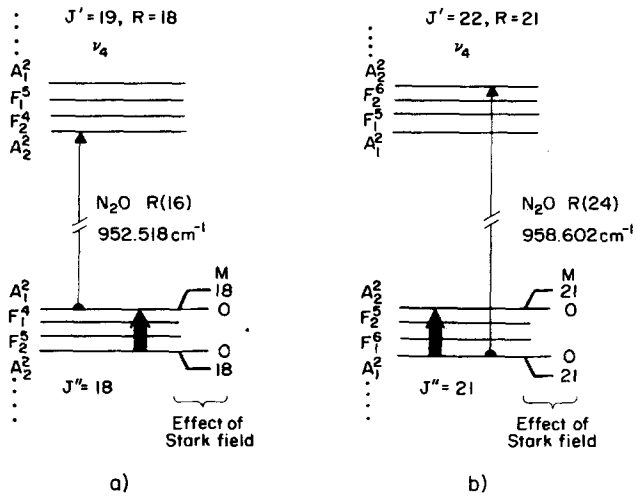

FIG. 5. Double resonance schemes for SiH_4. The heavy arrows indicate the rf transitions. The Stark effect for the component of highest M is indicated for the ground-state A_1–A_2 pairs. Note that the positive value of $\nu_M - \nu_L$ for the N_2O $R(16)$ laser line and the negative value of $\nu_M - \nu_L$ for the N_2O $R(24)$ laser line is consistent with the infrared assignments shown but with no others. If, for example, the SiH_4 infrared transition associated with N_2O $R(16)$ were ν_4 $R^-(18)$, $A_1^{(2)} \leftarrow A_2^{(2)}$ with $\nu_M - \nu_L$ positive, the second-order Stark effect would not shift the Stark components through the laser line.

uncertainties of less than 0.1 MHz even at the highest J values. It follows that quite definite assignments can be made from double resonances which involve these ground state splittings. The splittings in the $\nu_2 = 1$ and $\nu_4 = 1$ states are, however, known with much less accuracy, perhaps to ±100 MHz at best.

Connected to the N_2O $R(16)$ laser line an extremely strong rf line was detected at 993.02 ± 0.10 MHz. This is identified as the ground-state interval $J = 18$, $A_1^{(2)} - A_2^{(2)}$, which may be compared with 993.062 MHz calculated from the microwave work.[22] Although two much weaker double resonances associated with this laser line were detected earlier,[12] one of which was identified by Ozier *et al.* as the ground-state interval $J = 18$, $F_2^{(5)} - F_1^{(3)}$, we believe that the 993 MHz transition must be associated with the coincidence which gives rise to the laser Stark spectrum because of its intensity. For example, the 993 MHz line could be detected with 0.5 W rf power and 30 ms time constant, whereas for the two double resonances near 10 GHz an rf power greater than 10 W was required. We therefore assign the infrared transition as ν_4 $R^-(18)$, $A_2^{(2)} \leftarrow A_1^{(2)}$ of SiH_4, and we attribute the laser Stark spectrum as arising from the second-order Stark mixing of the ground-state levels $J = 18$, $A_1^{(2)}$, and $A_2^{(2)}$. The energy level scheme is shown in Fig. 5(a). The weak double resonance lines observed around 10 GHz are probably due to accidental near coincidences with other infrared transitions: the 10 239.78 MHz line identified as $J = 18$, $F_2^{(5)} \leftarrow F_1^{(3)}$ might possibly be associated with ν_4 $R^-(18)$, $F_2^{(3)} \leftarrow F_1^{(3)}$ of $^{29}SiH_4$ in 4.7% natural abundance.

The Stark effect on the 993 MHz double resonance line is shown in Fig. 6. For a first-order Stark effect a symmetrical splitting of the line would be expected, as was observed for GeH_4.[23] Instead we observe that the signal broadens and moves to higher frequency, which is consistent with the second-order Stark effect (see Fig. 5).

Connected with the N_2O $R(24)$ laser line we observed a double resonance signal at 859.01 ± 0.1 MHz. This is roughly one-tenth the intensity of the 993 MHz line. The 859 MHz line is assigned as the ground-state interval $J = 21$, $A_2^{(2)} \leftarrow A_1^{(2)}$, for which we calculate 859.09 MHz from the constants of Ozier *et al.* This confirms the assignment of the infrared transition suggested from the high-resolution infrared spectrum. The energy level scheme is shown in Fig. 5(b).

C. Stark effect calculations

Quantitative calculations of the Stark effect on the ground-state levels $J = 18$, $A_1^{(2)}$ and $J = 21$, $A_1^{(2)}$ were carried out. In each case the Stark coefficient $C(J, \kappa)$ for mixing of the A_1 level with the nearby $A_2^{(2)}$ level of the same J was computed by the method of Dorney and Watson,[19] using the appropriate eigenvector elements of a diagonalization of the ground-state rotational Hamiltonian in a $|Jkm\rangle$ basis of symmetric rotor functions referred to one of the S_4 axes of the molecule. We found that for the $J = 18$ A_1–A_2 pair $|C(J, \kappa)| = 17.605$, while for the $J = 21$ A_1–A_2 pair $|C(J, \kappa)| = 20.285$. Dorney and Watson noted that for the closely spaced bunches of levels at the upper limit of the energy manifolds, the $C(J, \kappa)$ approach the value of J with increasing J.

The Stark effects were then calculated by solving the 2×2 Stark matrices as a function of M and ϵ. θ_z^{xy} was given the value 3.34×10^{-5} D found by Kagann *et al.*[8] A detailed check confirmed that the influence of the $A_2^{(1)}$ levels, which are separated from the $A_1^{(2)}$ levels considered here by several GHz, is negligible. The results of the Stark effect calculations are given in Table I and Fig. 3, where they are compared with the experimental results.

IV. FURTHER EXPERIMENTAL OBSERVATIONS

One additional experiment to discriminate between first-order and second-order Stark effects was performed, an infrared double resonance experiment using modulation sidebands. This technique was developed by Brewer[24] and Luntz and Brewer[25] and it has been applied successfully to GeH_4.[9] The laser is amplitude modulated, so that sidebands are created (at ~ ± 1 MHz in our case). The modulated laser beam then passes through the external Stark cell. As the Stark field is increased from zero, a resonance occurs when the splitting between successive M components matches the modulation frequency (or half this frequency).[9]

This experiment was conducted for the N_2O $R(16)$ laser line. Instead of the simple spectrum with sharp resonances expected for a first-order Stark effect, similar to that observed for GeH_4,[9] we observed a broad unresolved hump. This indicates that the splittings between successive M components for a given field are not constant and, together with the continuous scan ex-

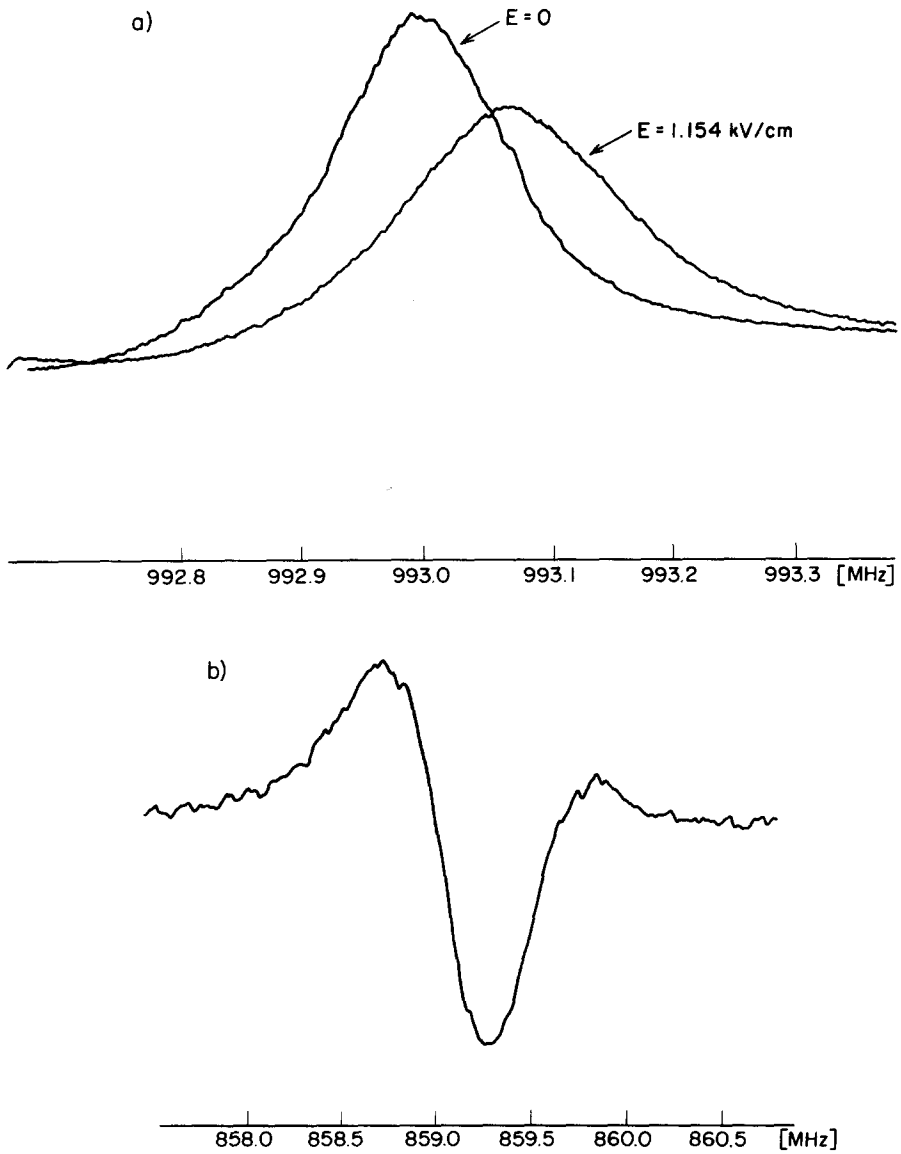

FIG. 6. Recordings of the ground-state rf transitions $J = 18\ A_1^{(2)} \leftarrow A_2^{(2)}$ at 993.02 MHz and $J = 21\ A_2^{(2)} \leftarrow A_1^{(2)}$ at 859.01 MHz. The traces of the 993 MHz line show the effect of a dc electric field of 1154 V/cm (mean value) applied to the waveguide cell. The broadening of the line and its shift to higher frequency are the behavior expected for a second-order Stark effect (see text and Fig. 5).

periment described earlier, confirms the presence of a second-order Stark effect.

We also report here several additional double resonances connected with laser lines other than N_2O $R(16)$ and $R(24)$. None of these near coincidences shows a laser Stark spectrum but it is convenient to summarize all the double resonance observations (including also those given earlier by Kreiner and Oka[12]) in this paper. In most cases the assignment of both the rf transition and the infrared transition can be made by comparison with the published results.[18,22] This information is given in Table II.

V. DISCUSSION

Since the second-order Stark effect in a nonpolar molecule is an unusual phenomenon, we have set out the evidence for our interpretation of the laser Stark spectrum in some detail. Examination of the energy level pattern for the ground vibrational state of tetrahedral molecules[20,22] shows that close A_1–A_2 pairs of energy levels which might have relatively fast second-order Stark effects are uncommon. They occur only at the top of the energy manifolds for every third J($J = 12, 15, 18, 21\ldots$) which always begin with the sequence A_1–F_1–F_2–A_2 or A_2–F_2–F_1–A_1. It is remarkable that in the few laser coincidences investigated for SiH_4, two laser lines have been found to strike a member of these A_1–A_2 pairs. Close F_1–F_2 pairs of energy levels are, however, much more common, and these may well provide candidates for the future observation of second-order Stark effects in tetrahedral molecules.

One of the most interesting points about our observations is that the experimental results can be explained satisfactorily on the basis of the Stark effect on the ground state alone. This is demonstrated by Fig. 2, although a small Stark effect of the upper state is presumably present but not detected with the present experimental resolution: a small upper state Stark effect could also improve the agreement of the calculated curve with the frequency offset measurements shown in Fig. 3. Nevertheless, any Stark shift in the upper state

TABLE II. Summary of assigned double resonances for SiH_4.

Laser line (cm^{-1})[a]		Infrared transition[b] Assignment	obs(cm^{-1})	calc(cm^{-1})	rf Transition[c] Assignment	obs(MHz)	calc(MHz)
N_2O $P(5)$,	934.647	ν_4 $R^-(9)$ $F_2^{(3)} \leftarrow F_1^{(3)}$	934.652	934.660	$J=9$ $F_2^{(2)} \leftarrow F_1^{(3)}$	170.26	170.105[d]
					$F_1^{(3)} \leftarrow F_2^{(4)}$	2279.48	2279.861[d]
N_2O $R(4)$,	942.975	ν_2 $P(5)$ $F_1^{(2)} \leftarrow F_2$	···	942.982	$J=5$ $F_1^{(2)} \leftarrow F_2$	185.68	185.611[d]
					$F_2 \leftarrow F_1^{(4)}$	60.69	60.466[d]
N_2O $R(16)$,	952.518	ν_4 $R^-(18)$ $A_2^{(2)} \leftarrow A_1^{(2)}$	952.530	952.534	$J=18$ $A_1^{(2)} \leftarrow A_2^{(2)}$	993.02	993.062
		^{29}Si ν_4 $R^-(18)$ $F_2^{(3)} \leftarrow F_1^{(3)}$?	···	~952.4[e]	$J=18$ $F_2^{(5)} \leftarrow F_1^{(3)}$	10239.78	10239.823[d]
N_2O $R(24)$,	958.602	ν_4 $R^-(21)$ $A_2^{(2)} \leftarrow A_1^{(2)}$	958.596	958.652	$J=21$ $A_2^{(2)} \leftarrow A_1^{(2)}$	859.01	859.088
$^{13}CO_2$ $R(14)$,	1028.512[f]	ν_4 $R^+(15)$ $F_1^{(2)} \leftarrow F_2^{(4)}$	···	1028.593	$J=15$ $F_2^{(4)} \leftarrow F_1^{(4)}$	321.36	321.357
$^{13}CO_2$ $P(40)$,	878.434[g]	^{29}Si ν_4 $P^+(8)$ $F_1^{(2)} \leftarrow F_2^{(2)}$?	···	~878.1[e]	$J=8$ $F_2^{(2)} \leftarrow F_1^{(2)}$	363.74	363.743
		^{30}Si ν_4 $P^+(8)$ $F_2^{(2)} \leftarrow F_1^{(2)}$?	···	~878.6[e]			
$^{13}CO_2$ $R(24)$,	931.309[g]	ν_2 $P(9)$ $F_1^{(1)} \leftarrow F_2^{(2)}$	931.298	931.312	$J=9$ $F_2^{(2)} \leftarrow F_1^{(3)}$	170.10	170.105[b]
$^{13}CO_2$ $R(26)$,	932.605[g]	ν_4 $Q^+(18)$ $F_2^{(4)} \leftarrow F_1^{(4)}$	···	932.555	$J=18$ $F_1^{(4)} \leftarrow F_2^{(5)}$	323.01	323.013

[a]Wave numbers of laser lines were taken from R. J. Whitford, K. J. Siemsen, H. D. Riccius, and G. R. Hanes, Opt. Commun. **14**, 70 (1975), and C. Freed, A. H. M. Ross, and R. G. O'Donnell, J. Mol. Spectrosc. **49**, 439 (1974).

[b]All transitions refer to the abundant isotopic species $^{28}SiH_4$ unless otherwise stated. Observed transitions are from Ref. 18, except that the $R^-(21)$ transitions are previously unreported.

[c]Calculated transitions are from Ref. 22.

[d]Discussed previously in Refs. 12, 18, and 22.

[e]The isotope shifts $\Delta\nu_4(^{28}Si-^{29}Si)$ and $\Delta\nu_4(^{28}Si-^{30}Si)$ are assumed to be about 1.3 cm^{-1} and 2.6 cm^{-1}, respectively. These isotope shifts have been measured precisely for the low J R branch region,[16] but isotope shifts in other parts of the band will be slightly different.

[f]9.8 μm band.

[g]10.9 μm band.

[h]A second double resonance observed at 458 MHz is almsot certainly the excited state transition $J'=8$, $\nu_2=1$, $F_2^{(2)} \leftarrow F_1^{(1)}$ (calc ~495 MHz).

must be roughly an order of magnitude smaller than in the ground state.

Two factors are involved in calculating the upper state Stark effect, the separation of the A_1–A_2 energy level pair and the size of the Stark matrix element connecting them. The energy level separations in the upper state are certainly somewhat larger than in the ground state, but not by an order of magnitude. For the upper state of the SiH_4 ν_4 $R^-(21)$ line, for example, the separation between $J'=22$, $R=21$, $A_1^{(2)}$, and $A_2^{(2)}$ is calculated to be ~1500 MHz. The multiplet in the infrared spectrum suggests that the prediction is underestimating the splitting, and that it may be ~3000 to 3500 MHz. These figures compare with the A_1–A_2 ground-state splitting of 859 MHz. It is difficult to avoid the conclusion that even though the upper state splitting is somewhat larger, the effective dipole moment in the upper state must be smaller than that in the ground state.

This conclusion is at first sight surprising. For GeH_4[9] the effective dipole moment operator in the upper state was found to be smaller by a factor of 9 than that in the lower state, and it appeared that the vibration-induced dipole moment must be cancelling the centrifugal distortion-induced dipole moment. There, however, the upper state belongs to the ν_2 band, which is vibrationally forbidden in the infrared and acquires its intensity only by Coriolis mixing with ν_4; thus a small value of the vibration-induced dipole moment seemed reasonable. In the case of SiH_4 the upper states of both infrared transitions belong to the infrared allowed ν_4 band, which would be expected to have a much larger vibration-induced dipole moment. Perhaps the explanation lies in the fact that the vibration-induced dipole moment in the $\nu_4=1$ state contains two terms,[26] one containing $\partial^2\mu_z/\partial Q_{4x}\partial Q_{4y}$ and the other $[\Phi_{4x4y3z}(\partial\mu_z/\partial Q_{3z})/\lambda_3 + \Phi_{4x4y4z}(\partial\mu_z/\partial Q_{4z})/\lambda_4]$ and it is of course possible for the resultant dipole moment to be small if there is accidentally a large degree of cancellation between these terms. There are so many unknowns in the expressions that we have not attempted to calculate the vibration-induced dipole moment at present.

ACKNOWLEDGMENTS

We wish to thank Dr. D. L. Gray for his assistance in running the vibration-rotation calculations and Dr. J. K. G. Watson, Dr. I. M. Mills, and Dr. A. R. W. McKellar for critical reading of this paper. One of us (W. A. K.) thanks the "Abteilung für Chemische Physik" of Ulm University for the loan of electronic equipment.

[1]T. Oka, *Molecular Spectroscopy: Modern Research*, edited by K. Narahari Rao (Academic, New York, 1976), Vol. II, p. 229.

[2]M. Mizushima and P. Venkateswarlu, J. Chem. Phys. **21**, 705 (1953).

[3]I. Ozier, Phys. Rev. Lett. **27**, 1329 (1971).

[4]J. K. G. Watson, J. Mol. Spectrosc. **40**, 536 (1971).

[5]T. Oka, F. O. Shimizu, T. Shimizu, and J. K. G. Watson,

Ap. J. Lett. **165**, L15 (1971).
[6]K. Fox, Phys. Rev. Lett. **27**, 233 (1971).
[7]M. R. Aliev, Sov. Phys.-JETP Lett. **14**, 417 (1971).
[8]R. H. Kagann, I. Ozier, and M. C. L. Gerry, J. Chem. Phys. **64**, 3487 (1976).
[9]W. A. Kreiner, B. J. Orr, U. Andresen, and T. Oka, Phys. Rev. A **15**, 2298 (1971).
[10]J. K. G. Watson, J. Mol. Spectrosc. **50**, 281 (1974).
[11]K. Uehara, J. Phys. Soc. Jpn. **34**, 777 (1975).
[12]W. A. Kreiner and T. Oka, Can. J. Phys. **53**, 2000 (1975).
[13]W. A. Kreiner, IEEE J. Quantum Electron. **12**, 16 (1976).
[14]S. M. Freund, G. Duxbury, M. Römheld, J. F. Tiedje, and T. Oka, J. Mol. Spectrosc. **52**, 38 (1974).
[15]J. W. C. Johns, A. R. W. McKellar, T. Oka, and M. Römheld, J. Chem. Phys. **62**, 1488 (1975).
[16]J. W. C. Johns, W. A. Kreiner, and J. Susskind, J. Mol. Spectrosc. **60**, 400 (1976).
[17]J. Susskind, J. Chem. Phys. **56**, 5152 (1972).
[18]D. L. Gray, A. G. Robiette, and J. W. C. Johns, Mol. Phys. (to be published).
[19]D. L. Gray and A. G. Robiette, Mol. Phys. **32**, 1609 (1976).
[20]A. J. Dorney and J. K. G. Watson, J. Mol. Spectrosc. **46**, 135 (1972).
[21]T. Oka, *Frontiers in Laser Spectroscopy*, Les Houches Summer School Proceedings, Session XXVII, edited by R. Balian, S. Haroche, and S. Liberman (North Holland, Amsterdam, (1977).
[22]I. Ozier, R. M. Lees, and M. C. L. Gerry, Can. J. Phys. **54**, 1094 (1976).
[23]W. A. Kreiner, U. Andresen, and T. Oka, J. Chem. Phys. **66**, 4662 (1977).
[24]R. G. Brewer, Phys. Rev. Lett. **25**, 1639 (1970).
[25]A. C. Luntz and R. G. Brewer, J. Chem. Phys. **54**, 3641 (1971).
[26]I. M. Mills, J. K. G. Watson, and W. L. Smith, Mol. Phys. **16**, 329 (1969).